Nucleon-nucleus inelastic scattering using a relativistic impulse approximation with exchange

E. Rost and J. R. Shepard
Department of Physics, University of Colorado, Boulder, Colorado 80309
(Received 29 September 1986)

We formulate a microscopic relativistic treatment of nucleon-nucleus inelastic scattering in a distorted wave impulse approximation. The interaction is taken from a Lorentz invariant formulation with explicit direct *and* exchange terms constrained by fitting to experimental NN amplitudes. This procedure allows us to apply the theory in the lower range of intermediate energies (100—400 MeV) where exchange effects are likely to be important. Application to inelastic scattering uses this interaction for both the distorting potentials and the transition interaction. Effects of explicit exchange are studied and a preliminary analysis of ^{12}C(p,p') data is presented.

I. INTRODUCTION

Relativistic models of nucleon-nucleus scattering have usually been restricted to elastic scattering. At high energies ($\gtrsim$400 MeV) it is possible to construct a relativistic impulse approximation (RIA) so that the p-A elastic amplitude is obtained without adjustable parameters from NN and (e,e) data alone.[1,2] The theory has been generalized to give macroscopic[3] (collective) and microscopic[4] models of the inelastic scattering reaction. In all these treatments, the projectile has been treated as distinguishable from the target nucleons, i.e., *explicit* knockon exchange terms are ignored. [However, a similar truncation occurs in fitting NN data for the impulse approximation so some effects of exchange (i.e., *nonexplicit*) were present in the earlier treatments.] As will be discussed below, the effects of explicit exchange are expected to be small at high energy where the overlap between bound and projectile wave functions is small.

It is of interest to extend the treatment of p-A scattering to lower energies ($\sim$100—400 MeV) for several reasons; the nucleus is more transparent at these lower energies, experimental data are easier to obtain, and one would like to see where and how the impulse approximation breaks down. In this endeavor it is important to treat nucleon (i.e., knockon) exchange explicitly since it is known that without such a treatment the scalar and vector optical potentials diverge as the energy is lowered (the values at 100 MeV are much greater in magnitude than phenomenology[5] requires.) Fortunately a framework for handling exchange explicitly has been given by Horowitz,[6] who has constructed an antisymmetrized Lorentz invariant NN amplitude in a "meson" model. Optical potentials generated from these amplitudes then contain an exchange term, and the resulting effective potentials do *not* diverge at lower energy, and give a good description of elastic scattering data in the 100—400 MeV energy range.[7]

However, we note that the direct contribution to elastic scattering mostly involves only the $T=0$ scalar and vector part of the NN interaction while pion exchange dominates the exchange contribution. It has been shown elsewhere[8] that *inelastic* scattering in a relativistic framework can in general depend on all pieces of the interaction and that the selection rules governing a specific process can emphasize various of these. Thus extensions of the RIA approach to inelastic scattering will allow more stringent tests of the model than those posed by elastic scattering.

In Sec. II, we present the theoretical formulation of the RIA with exchange using a helicity expansion[9] of the wave functions. The model is studied in Sec. III, where the effects of exchange are examined in detail. The full distorted wave RIA calculations are then compared to experimental data for the lowest 1^+ and 2^+ levels in ^{12}C (both $T=0$ and $T=1$). Our conclusions are found in Sec. IV.

II. THEORETICAL FORMULATION

We wish to calculate the transition amplitude for nucleon-nucleus inelastic scattering in the framework of a relativistic distorted wave impulse approximation with an *explicit* treatment of exchange (DREX). We consider a process in which a nucleus is excited from an initial state $\Psi_{J_iM_i}$ to a final state $\Psi_{J_fM_f}$. We then take the transition amplitude to be

$$T_{fi}=\sum_{n=1}^{A}\psi^{(-)\dagger}_{\mathbf{k}'s'}\Psi^{\dagger}_{J_fM_f}\gamma^0(0)\gamma^0(n)\hat{t}(0,n)\psi^{(+)}_{\mathbf{k}s}\Psi_{J_iM_i}\,, \tag{2.1}$$

where integration over the A target nucleons and the projectile (0) is implied. The projectile wave functions, $\psi^{(\mp)}_{\mathbf{k}s}$, have boundary conditions specified by $(-)$ or $(+)$ and asymptotic momentum and spin projection indicated by $\mathbf{k}$ and s, respectively; the nuclear wave functions Ψ_{JM} are functions of the coordinates of all A constituent nucleons. In Eq. (2.1), γ^0 is the usual timelike vector Dirac matrix and $\hat{t}$ is the relativistic invariant form of the nucleon-nucleon interaction which drives the transition. Unlike a similar expression in Ref. 4, the operator $\hat{t}$ here contains explicit direct *and* exchange terms.

In impulse approximation, the operator $\hat{t}$ becomes

$$\hat{t}\rightarrow\frac{-8\pi i}{E_{\rm NN}}p_{\rm NN}\hat{F}\ , \tag{2.2}$$

where $p_{\rm NN}$ and $E_{\rm NN}$ are the nucleon momentum and total energy, respectively, in the NN center-of-momentum frame. The operator $\hat{F}$ is generated from a free NN amplitude evaluated at a fixed asymptotic value $s_0=(p_1+p_2)^2$. Then following the development of Eqs. (1)—(9) of Ref. 4, we arrive at the expression

$$\begin{aligned}T_{fi}=\frac{-8\pi i}{E_{\rm NN}}p_{\rm NN}\sum_{n=1}^{A}\sum_{I_{\rm NN}}\int dx\,dy_n\psi^{(-)\dagger}_{\mathbf{k}'s'}(x)\Psi^{\dagger}_{J_fM_f}(y_1,\ldots,y_A)\gamma^0(0)\gamma^0(n)\\ \times[\hat{F}(s_0,|x-y_n|)\psi^{(+)}_{\mathbf{k}s}(x)\Psi_{J_iM_i}(y_1,\ldots,y_n,\ldots,y_A)\\ +(-1)^{I_{\rm NN}}\hat{F}(s_0,|x-y_n|)\psi^{(+)}_{\mathbf{k}s}(y_n)\Psi_{J_iM_i}(y_1,\ldots,x,\ldots,y_A)]\ ,\end{aligned} \tag{2.3}$$

where $I_{\rm NN}$ denotes the isospin of the $(0,n)$ nucleon-nucleon system (the amplitude $\hat{F}$ also depends implicitly on this isospin quantity). The second term in Eq. (2.3) has exchanged the x and y_n labels in the initial state and thus treats the *explicit* change of the projectile and target nucleon. We now present a detailed specification of the interaction $\hat{F}$, the distorted waves ψ, and the bound state functions Ψ emphasizing those features which differ from the nonrelativistic formulation.

A. The interaction $\hat{F}$

Recent applications[6,7] of the Dirac impulse approximation to elastic scattering utilize an expansion of the NN amplitude in terms of the local relativistic covariants

$$\begin{aligned}\hat{F}=\hat{F}_S+\gamma(1)\cdot\gamma(2)\hat{F}_V+\gamma^5(1)\frac{\boldsymbol{q}}{2M}(1)\gamma^5(2)\frac{\boldsymbol{q}}{2M}(2)\hat{F}_P\\ +\gamma^5(1)\gamma^5(2)\gamma(1)\cdot\gamma(2)\hat{F}_A+\sigma^{\mu\nu}(1)\sigma_{\mu\nu}(2)\hat{F}_T\ ,\end{aligned} \tag{2.4}$$

where the various $\hat{F}_j$ are complex functions of kinematic variables obtained by equating the Dirac free spinor matrix elements of (2.4) to the NN amplitudes using the prescription

$$\begin{aligned}\bar{U}_1\bar{U}_2\hat{F}U_1U_2=A+B\boldsymbol{\sigma}(1)\cdot\boldsymbol{\sigma}(2)+iqC[\boldsymbol{\sigma}(1)\cdot\hat{\mathbf{n}}+\boldsymbol{\sigma}(2)\cdot\hat{\mathbf{n}}]\\ +D\boldsymbol{\sigma}(1)\cdot\hat{\mathbf{q}}\boldsymbol{\sigma}(2)\cdot\hat{\mathbf{q}}+E\boldsymbol{\sigma}(1)\cdot\hat{\mathbf{z}}\boldsymbol{\sigma}(2)\cdot\hat{\mathbf{z}}\ ,\end{aligned} \tag{2.5}$$

where A, B, C, D, and E are the Wolfenstein amplitudes[10] which are obtained in phase-shift analyses[11] of NN scattering.

For calculational purposes it is convenient to express Eq. (2.4) in terms of matrices Γ_ν which connect upper and lower components, viz.,

$$\begin{aligned}\gamma^0(1)\gamma^0(2)\hat{F}(|x-y|)\\ =\sum_{\nu=1}^{4}[f^\nu(|x-y|)+g^\nu(|x-y|)\boldsymbol{\sigma}(1)\cdot\boldsymbol{\sigma}(2)]\\ \times\Gamma_\nu(1)\Gamma_\nu(2)\ ,\end{aligned} \tag{2.6}$$

where

$$\Gamma_1=\begin{bmatrix}1&0\\0&1\end{bmatrix},\quad \Gamma_2=\begin{bmatrix}1&0\\0&-1\end{bmatrix},\quad \Gamma_3=\begin{bmatrix}0&1\\1&0\end{bmatrix},\quad \Gamma_4=\begin{bmatrix}0&1\\-1&0\end{bmatrix} \tag{2.7}$$

and

$$\begin{aligned}f^1=F_V,\ f^2=F_S,\ f^3=F_A,\ f^4=F_P\ ,\\ g^1=-F_A,\ g^2=2F_T,\ g^3=-F_V,\ g^4=2F_T\ .\end{aligned} \tag{2.8}$$

The detailed specification of the $\hat{F}_j$ quantities follows the work of Horowitz, who writes[6] in momentum space

$$\hat{F}_j=i\frac{E_{\rm NN}}{2p_{\rm NN}}[\hat{F}_j^{(D)}(q)+\hat{F}_j^{(X)}(Q)]\ , \tag{2.9}$$

where q and Q are the direct and exchange momentum transfers, respectively. The direct term is decomposed as

$$\begin{aligned}\hat{F}_j^{(D)}=h_j^{(0)}(q)+\boldsymbol{\tau}(1)\cdot\boldsymbol{\tau}(2)h_j^{(1)}(q)\ ,\\ h_j^{(I)}(q)=\frac{g_{Ij}^2}{q^2+m_{Ij}^2}\left[1+\frac{q^2}{\Lambda_{Ij}^2}\right]^{-2}\\ -i\frac{\tilde{g}_{Ij}^2}{q^2+\tilde{m}_{Ij}^2}\left[1+\frac{q^2}{\tilde{\Lambda}_{Ij}^2}\right]^{-2}\ ,\end{aligned} \tag{2.10}$$

with a similar decomposition for the exchange term.[6] Thus there are six parameters for each of the 10 (Ij) "mesons."

For our inelastic scattering calculations, we require a configuration space representation which is

$$\begin{aligned}h(r)=\frac{g^2}{4\pi}\frac{\Lambda^2}{\Lambda^2-m^2}\\ \times\left[\frac{\Lambda^2}{\Lambda^2-m^2}\left[\frac{e^{-mr}}{r}-\frac{e^{-\Lambda r}}{r}\right]-\frac{\Lambda}{2}e^{-\Lambda r}\right]\ .\end{aligned} \tag{2.11}$$

A multipole expansion of Eq. (2.11) may be worked out, yielding

$$h(|r_1-r_2|)=\frac{g^2}{4\pi}\sum_L (2L+1)V_L(r_1,r_2)P_L(\hat{\mathbf{r}}_1\cdot\hat{\mathbf{r}}_2)\ , \tag{2.12}$$

with

$$V_L(r_1,r_2)=\sum_{\lambda=1}^{4} A_\lambda F_\lambda(r_<)H_\lambda(r_>)\ , \tag{2.13}$$

where $r_<$ ($r_>$) is the lesser (greater) of r_1,r_2 and

$$A_1=m\left[\frac{\Lambda^2}{\Lambda^2-m^2}\right]^2,\quad A_2=\frac{\Lambda^3}{2(\Lambda^2-m^2)}-\frac{\Lambda^5}{(\Lambda^2-m^2)^2},\quad A_3=A_4=\frac{\Lambda^3}{2(\Lambda^2-m^2)}\ . \tag{2.14}$$

The F and H functions in Eq. (2.13) are defined by

$$\begin{aligned} &F_1(r)=i_L(mr),\quad F_2(r)=i_L(\Lambda r)\ ,\\ &F_3(r)=\Lambda r i_L'(\Lambda r),\quad F_4(r)=i_L(\Lambda r)\ ,\\ &H_1(r)=k_L(mr),\quad H_2(r)=k_L(\Lambda r)\ ,\\ &H_3(r)=k_L(\Lambda r),\quad H_4(r)=\Lambda r k_L'(\Lambda r)\ , \end{aligned} \tag{2.15}$$

with

$$i_L(x)=\sqrt{\pi/(2x)}I_{L+1/2}(x)\ ,\qquad k_L(x)=\sqrt{\pi/(2x)}K_{L+1/2}(x)$$

in terms of the modified Bessel functions.[12]

Evaluation of the transition matrix elements, Eq. (2.1), is efficiently accomplished using a helicity representation for the operators and wave functions involved. Thus a term in Eq. (2.6) is written

$$f^{\nu}(|x-y|)\rightarrow(2J+1)V_J(x,y)\Gamma_1(1)\Gamma_1(2) \tag{2.16}$$

for a "central" term while we find

$$\begin{aligned} g^{\nu}(|x-y|)\boldsymbol{\sigma}(1)\cdot\boldsymbol{\sigma}(2)\rightarrow&-(2J+1)V_J(x,y)\Gamma_3(1)\Gamma_3(2)+[JV_{J-1}(x,y)+(J+1)V_{J+1}(x,y)]\Gamma_2(1)\Gamma_2(2)\\ &+[(J+1)V_{J-1}(x,y)+JV_{J+1}(x,y)]\Gamma_4(1)\Gamma_4(2)+\sqrt{J(J+1)}[V_{J-1}(x,y)-V_{J+1}(x,y)]\Gamma_2(1)\Gamma_4(2) \end{aligned} \tag{2.17}$$

for a "spin-spin" term where the helicity operators are given in Eq. (2.7) but here act in spin space rather than upper-lower component space. They operate on orthonormal helicity functions $|\lambda\rangle$ with projection $\lambda=\pm\frac{1}{2}$ along the *radial* direction i.e., $\hat{x}$ for (1) and $\hat{y}$ for (2).

B. The distorted waves ψ

A four-component distorted wave with spin projection s along a fixed quantization axis $\mathbf{k}$ may be written as

$$\psi_{\mathbf{k}s}(\mathbf{r})=\frac{4\pi}{kr}\sum_{JL\mu\sigma'}(L\tfrac{1}{2}\mu s\,|\,J\mu+s)Y_L^{\mu}(\hat{\mathbf{k}})\begin{bmatrix} U_{LJ}(r)(L\tfrac{1}{2}\mu'\sigma'\,|\,J\mu+s)Y_L^{\mu}(\hat{\mathbf{r}})\,|\,\sigma'\rangle \\ W_{LJ}(r)(L'\tfrac{1}{2}\mu'\sigma'\,|\,J\mu+s)Y_{L'}^{\mu}(\hat{\mathbf{r}})\,|\,\sigma'\rangle \end{bmatrix}, \tag{2.18}$$

where $L'=2J-L$, $\mu'=\mu+s-\sigma'$, and $|\sigma'\rangle$ is the spin projection at point $\mathbf{r}$ along this fixed axis. This may be rotated to helicity spin functions $|\lambda'\rangle$ (with projection along $\mathbf{r}$) using rotation functions

$$|\sigma'\rangle=\sum_{\lambda'}D^{*(1/2)}_{\sigma'\lambda'}(\phi_r\theta_r\psi_r)\,|\lambda'\rangle\ , \tag{2.19}$$

where $(\phi_r\theta_r\psi_r)$ are Euler angles relating $\hat{\mathbf{r}}$ to $\hat{\mathbf{k}}$. We then express $Y_L^{\mu'}(\hat{\mathbf{r}})$ in terms of the rotation functions, use explicit forms of the vector coupling coefficients, and find after some algebra

$$\psi^{(+)}_{\mathbf{k}s}(\mathbf{r})=\frac{(2\pi)^{-1/2}}{kr}\sum_{J\lambda'}(J+\tfrac{1}{2})D^{*J}_{s\lambda'}(\phi_r\theta_r\psi_r)\begin{bmatrix}[U_<(r)+(-1)^{s-\lambda'}U_>(r)]\,|\,\lambda'\rangle \\ [(-1)^{\lambda'+1/2}W_<(r)+(-1)^{s+1/2}W_>(r)]\,|\,\lambda'\rangle\end{bmatrix}, \tag{2.20}$$

where $U_<$ denotes $U_{L=J-1/2,J}$, etc. [Note that the phases of these radial functions are defined by Eq. (2.18) and contain an i^l and Coulomb phase for convenience.]

The helicity expansion of the "ingoing" distorted wave is similarly obtained and yields

$$\psi^{(-)*}_{\mathbf{k}'s'}(\mathbf{r})=\frac{(2\pi)^{-1/2}}{kr}\sum_{J\lambda'}(J+\tfrac{1}{2})D^{J}_{s'\lambda'}(\tilde{\phi}_r\tilde{\theta}_r\tilde{\psi}_r)\begin{bmatrix}[\tilde{U}_<(r)+(-1)^{s'-\lambda'}\tilde{U}_>(r)]\,|\,\lambda'\rangle \\ [(-1)^{\lambda'+1/2}\tilde{W}_<(r)+(-1)^{s'+1/2}\tilde{W}_>(r)]\,|\,\lambda'\rangle\end{bmatrix}, \tag{2.21}$$

where the angles $(\tilde{\phi}_r\tilde{\theta}_r\tilde{\psi}_r)$ fix $\hat{\mathbf{r}}$ and $\hat{\mathbf{k}}'$ and $\tilde{U},\tilde{W}$ are radial functions appropriate for the final state ejectile.

C. The bound state functions Ψ

For simplicity we will consider a single particle-hole transition, $\Psi_{J_iM_i}=|0\rangle$ and

$$\Psi_{J_fM_f}=[a^\dagger_{j_p}\tilde{a}_{j_h}]_{J_fM_f}|0\rangle$$

in the notation of Ref. 4. Then integration over the spectator nucleons leaves us with the four-component wave functions

$$|j_pm_p\rangle=\frac{\sqrt{2j_p+1}}{4\pi}\sum_\lambda D^{*j_p}_{m_p\lambda}(\phi_r\theta_r\psi_r)\begin{bmatrix}u^{j_p}_\lambda(r)|\lambda\rangle\\ iw^{j_p}_\lambda(r)|\lambda\rangle\end{bmatrix}, \tag{2.22}$$

$$\langle j_hm_h|=\frac{\sqrt{2j_h+1}}{4\pi}\sum_\lambda D^{j_h}_{m_h\lambda}(\phi_r\theta_r\psi_r)\begin{bmatrix}\langle\lambda|\tilde{u}^{j_h}_\lambda(r)\\ -i\langle\lambda|\tilde{w}^{j_h}_\lambda(r)\end{bmatrix}, \tag{2.23}$$

where

$$\begin{aligned}&u^j_{1/2}(r)=(-1)^{l+j-1/2}g_{lj}(r),\quad u^j_{-1/2}(r)=g_{lj}(r),\\ &w^j_{1/2}(r)=-(-1)^{l+j-1/2}f_{lj}(r),\quad w^j_{-1/2}(r)=f_{lj}(r),\end{aligned} \tag{2.24}$$

in terms of the usual[13] radial wave functions g and f for upper and lower components of the particle orbital (the hole orbital is denoted with a tilde). Generalization to cases with several particle-hole components or to nonzero J_i is straightforward.

D. Evaluation of the transition amplitude

The transition amplitude is evaluated by inserting the bound state, distorted wave, and interaction into Eq. (2.3) and performing standard traces to obtain observables of interest. The innermost part of the calculation consists of the evaluation of integrals of the general form of

$$\int dr_1\int dr_2\tilde{C}(r_1)\tilde{B}(r_2)F(r_<)H(r_>)C(r_1)B(r_2) \tag{2.25}$$

for the direct part and

$$\int dr_1\int dr_2\tilde{C}(r_1)\tilde{B}(r_2)F(r_<)H(r_>)C(r_2)B(r_1) \tag{2.26}$$

for the exchange part. In the above integrals, B $(\tilde{B})$ denotes a bound radial function (either upper or lower) for the initial (final) state and C $(\tilde{C})$ denotes similar radial functions for the continuum distorted waves. The helicity formulation allows for substantial economy in the evaluation of these integrals. Except for the bookkeeping in working out the upper-lower terms in Eq. (2.6), the procedure is the same as outlined by Raynal[9] and will not be repeated here. The presence of lower components requires us to compute roughly four times as many terms as in a nonrelativistic case. On the other hand, the complicated tensor and spin-orbit interaction terms of a nonrelativistic treatment do not appear.

The computations are made feasible on a minicomputer (e.g., VAX 11/780) by storing on disk the radial arrays of multipoles [Eq. (2.15)], distorted radial wave functions [Eqs. (2.20) and (2.21)], and bound radial functions [Eq. (2.24)]. Typical running times are then about one hour, which is about two times longer than for a comparable nonrelativistic calculation (DW81).[14]

E. Calculational checks

It is crucial to subject a complicated computer code to a series of tests. Obvious checks were comparisons with the nonrelativistic helicity code DW81 (Ref. 14) and comparison to a fixed spin-axis relativistic code DRIA (Ref. 4) with exchange terms omitted from DREX. A further check of the spin algebra is possible when short-range interactions are used (so that the folding becomes a simple factor). In this case one can write the Dirac matrix content of the exchange interaction for type $j(=S,V,P,A,T)$ as

$$\lambda^j_{12'}\lambda^j_{21'}=\sum_k C_{jk}\lambda^k_{11'}\lambda^k_{22'}, \tag{2.27}$$

where the C_{jk} are Fierz coefficients (see Ref. 6 for details). The right-hand side (rhs) may then be evaluated in the "direct" code DRIA and cases with both direct and exchange contributions can be handled by a simple generalization of Eq. (2.27). The code DREX has passed these and other tests.

III. RESULTS

In this section we will explore the effects of explicit exchange in Dirac impulse approximation calculations of proton inelastic scattering. We treat as a prototype reaction p-shell excitations in ^{12}C. The orbitals are generated from a potential well of Woods-Saxon shape with radius $1.27\times(12)^{1/3}$ fm and diffusivity 0.635 fm—parameters which yield proton orbitals consistent with electron scattering data. Initial strengths of -430 MeV and $+361$ MeV were assumed for the scalar and timelike vector potentials. Their sum was adjusted by a factor of 0.965 (0.975) to fit the experimental separation energies of 15.4 MeV (9.7 MeV) for the $p_{3/2}$ ($p_{1/2}$) orbitals. This approach results in wave functions and potentials very similar to those obtained in the relativistic Hartree approach of Horowitz and Serot.[15]

Distorted waves were generated from an optical potential derived in the relativistic impulse approximation using the same relativistic invariants [Eq. (2.4)] as are used at the inelastic vertex. The potential for elastic scattering also includes medium modifications from Pauli blocking calculated in a local density approximation with knockon exchange included.[6,7] The density distribution in configuration space was taken from a three-parameter Fermi fit[16] to electron scattering data, viz., ($r_0=1.029$ fm, $a=0.5224$ fm, and $w=-0.149$ fm). When inserted into the Dirac equation, this optical potential yields a good description of ^{12}C elastic scattering cross section and analyzing power data at intermediate energies.[7] It therefore provides an internally consistent and quantitatively

accurate procedure for generating distorted waves for use in the inelastic scattering calculations to be described.

As an initial study we examine in Fig. 1 the energy dependence of some experimental observables for an idealized ^{12}C(p,p') excitation of a pure $p_{3/2}^{-1}p_{1/2}$ configuration. We have chosen the maximally sensitive $J=1$, $T=1$ excitation to demonstrate the effect of exchange. The calculations were performed at energies of 135, 200, and 400 MeV where explicitly antisymmetrized relativistic NN amplitudes are available.[6] The calculations compare explicit exchange (DREX—solid line) with implicit exchange (DRIA—dotted line); all other aspects of the calculation including distortion were kept the same. It is seen that the differential cross sections are less sensitive to the treatment of exchange than the spin observables in this regard. Also the effects due to explicit exchange become smaller at the higher energies, as we would expect from general considerations to be discussed below.

In the remaining discussion we shall consider physical ^{12}C(p,p') transitions and will compare our calculations to existing data. This will be done for excitation of the 4.43 MeV ($J=2$, $T=0$), 16.11 MeV ($J=2$, $T=1$), 12.71 MeV ($J=1$, $T=0$), and 15.11 MeV ($J=1$, $T=1$) levels. We will use nuclear structure amplitudes given by the Lee and Kurath[17] nonrelativistic shell-model calculation although we realize that such amplitudes are not consistent with our relativistic model. We have modified the Lee and Kurath amplitude for the 1^+, $T=0$ excitation by dropping the $L=1$, $S=0$ amplitude. This amplitude governs the convection current contribution to the excitation process, and the justification for omitting it is discussed in detail in Ref. 8.

Figure 2 shows the relativistic distorted wave impulse approximation calculations with explicit treatment of exchange (DREX) for the natural parity 2^+, $T=0$ excitation at 200 MeV incident proton energy. The normalization is taken from electron scattering [i.e., the calculation using the Cohen-Kurath p-shell wave functions[17] is multiplied by a factor of 2 for the collective state as required by (e,e') scattering data—calculations for the other levels are not renormalized]. Also shown in Fig. 2 are distorted-wave impulse approximation calculations where the effects of exchange are included implicitly (DRIA) in the parametrization of the NN amplitudes[18] and therefore also in the (p,p') calculation itself. The dashed curve in the figure presents the (DREX) calculation with the exchange term omitted. This calculation has no physical significance *vis à vis* the data but does allow us to examine the relative importance of calculated exchange terms.

Figure 2 shows excellent agreement of both DREX and DRIA calculations with the 2^+, $T=0$ cross section and analyzing power data.[14] The figure also shows that the DREX exchange contribution is appreciable. However, the DREX and DRIA results are nearly identical, suggesting that *explicit* treatment of exchange is not important for this transition. We may qualitatively understand such a result by examining the plane-wave exchange matrix element [i.e., the second term of Eq. (2.3)]. In momentum space the (local) NN t matrix is written as

$$t_{\mathrm{NN}} \rightarrow t_{\mathrm{NN}}(q_x^2) , \tag{3.1}$$

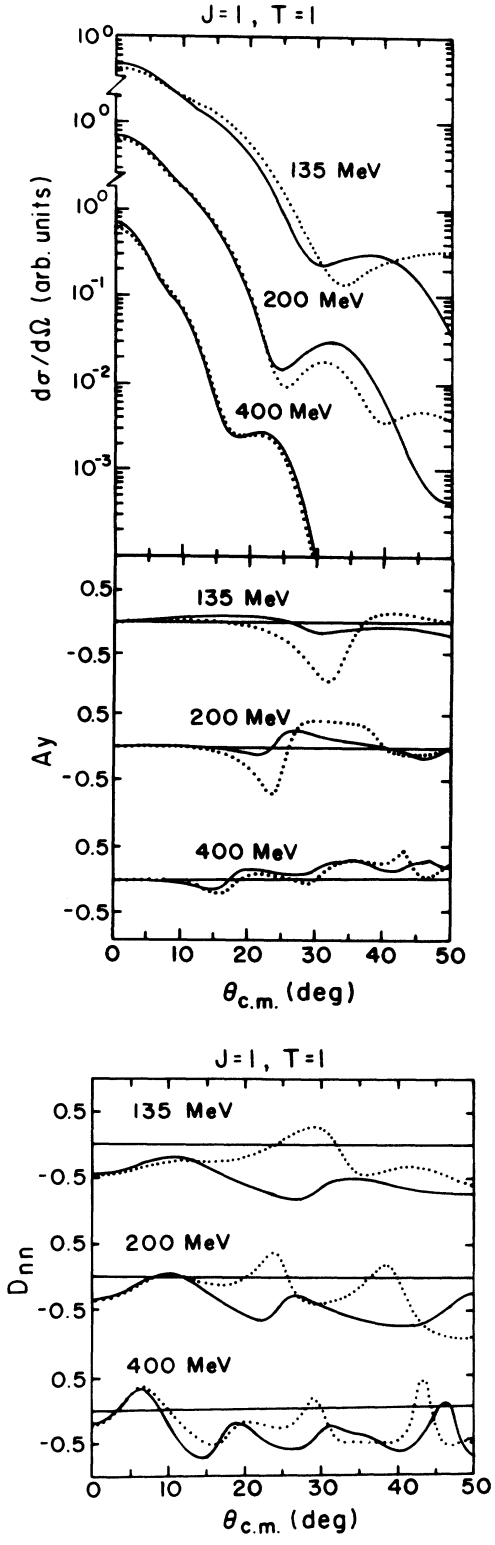

FIG. 1. Cross sections and analyzing powers for excitation of an idealized ($J=1, T=1$) level in ^{12}C by protons of 135, 200, and 400 MeV incident energy. The solid line curves were calculated with the full explicit-exchange code DREX; the dotted curves were calculated without explicit exchange (code DRIA) as described in Ref. 4.

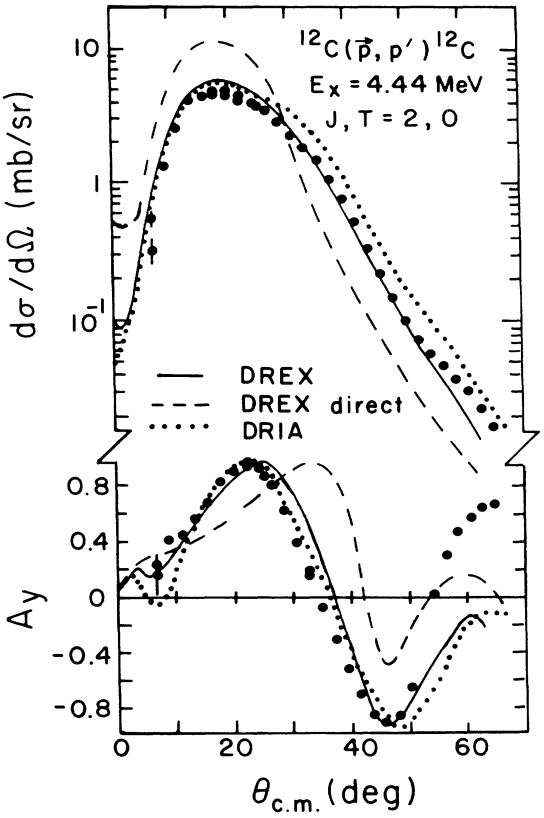

FIG. 2. Relativistic DREX calculations (solid line) are compared with the data from Ref. 14 for excitation of the 4.44 MeV 2^+, $T=0$ state in ^{12}C by 200 MeV protons. Also shown are DREX calculations with only a direct term (dashed line) and a nonexplicit exchange DRIA calculation (dotted line).

where the *exchange* momentum transfer is $\mathbf{q}_x=\mathbf{p}_f-\mathbf{k}_i=\mathbf{p}_i-\mathbf{k}_f=\mathbf{p}-\mathbf{k}$ and where $\mathbf{p}_i$ ($\mathbf{p}_f$) is the initial (final) projectile momentum and $\mathbf{k}_i$ ($\mathbf{k}_f$) is the initial (final) momentum of the bound nucleon, while $\mathbf{p}\equiv\frac{1}{2}(\mathbf{p}_i+\mathbf{p}_f)$ and $\mathbf{k}\equiv\frac{1}{2}(\mathbf{k}_i+\mathbf{k}_f)$. We note that $\mathbf{k}_i$, $\mathbf{k}_f$, and $\mathbf{k}$ are *operators* in the target space. We now expand $t_{\rm NN}(q_x^2)$ about $\mathbf{k}=0$:

$$t_{\rm NN}(q_x^2)=t_{\rm NN}[(\mathbf{p}-\mathbf{k})^2]$$
$$\simeq t_{\rm NN}(p^2)\left[1-\frac{2}{t_{\rm NN}(p^2)}\frac{\partial t_{\rm NN}}{\partial p^2}\mathbf{p}\cdot\mathbf{k}\right]. \quad (3.2)$$

The first term on the rhs does not depend on $\mathbf{k}$. Therefore the *dynamical* dependence of this piece of $t_{\rm NN}(q_x^2)$ can be factored out of the target matrix element and, after a Fierz transformation [Eq. (2.27)], has a form identical to that of the direct term. This implies that the exchange contribution associated with this first term can be included *implicitly* via an effective direct-only NN t matrix. This is essentially what is done in the code DRIA. The second term of the expansion, which we call a "current-current" contribution since $\mathbf{p}$ and $\mathbf{k}$ are proportional to the projectile and target nucleon convection currents, respectively, contains $\mathbf{k}$, a dynamical operator in the target space which cannot be factored. Consequently, its contribution—which is implicitly included in the DREX exchange amplitude—is absent in DRIA calculations. We note that in standard nonrelativistic treatments of (p,p'), current-current contributions arising from exchange processes are the only source of convection current or composite current terms when a local form of the NN t matrix is used. Composite current terms are required to give nonzero $P-A_y$.[19,20] The qualitative physical behavior of the current-current term is most easily understood by assuming that $t_{\rm NN}$ has the form of a static one-boson-exchange potential

$$t_{\rm NN}(q_x^2)\rightarrow\frac{g^2}{q_x^2+\mu^2}\simeq\frac{g^2}{p^2+\mu^2}\left[1+\frac{2}{p^2+\mu^2}\mathbf{p}\cdot\mathbf{k}\right]. \quad (3.3)$$

The current-current term vanishes in two specific limits: One such limit is $\mu\rightarrow\infty$. This is reasonable since $\mu\rightarrow\infty$ implies a zero-range potential in configuration space, in which case the exchange integral can readily be cast in the same form as the direct. Another such limit is $p\gg k$, roughly corresponding to a projectile kinetic energy much greater than the Fermi energy ($\sim$40 MeV). The energy dependence of the relative importance of exchange as demonstrated in Fig. 1 is consistent with such a picture. We then conclude that the similarity between the DREX and DRIA calculations appearing in Fig. 2 means that contributions arising from the first term on the rhs of Eqs. (3.2) and (3.3) are dominant in the exchange integrals and that the current-current contributions are small. Since at 200 MeV we are not yet in the $p\gg k$ regime, this is equivalent to saying that the terms of $t_{\rm NN}$ which are dominant in the exchange integrals are of *short* range. This of course effectively excludes the pionic contribution, which test calculations show is, indeed, quite small in this case.

Figure 3 compares DREX and DRIA calculations with 200 MeV cross sections and analyzing power data for the 16.11 MeV 2^+, $T=1$ level. In contrast to the 2^+, $T=0$ transition, the excitation of this level is dominated by the spin-dependent terms in the NN t matrix [Eq. (2.5)]. Here the full DREX calculation is again in excellent agreement with the experimental cross section. It may be noted that the shapes of the differential cross sections are different for the 2^+, $T=0$ and $T=1$ cases and that this difference is accurately reproduced by DREX. However, the analyzing power data for the $T=1$ transition are only qualitatively reproduced by the DREX results. Figure 3 also reveals that exchange is relatively more important for the $T=1$ case, both in the sense that it makes a larger relative contribution in the DREX calculations and also insofar as the DREX vs DRIA differences are greater, with DREX providing distinctly superior agreement with data. In the context of the above discussion, we interpret the increased DREX vs DRIA differences to mean that the current-current terms on the rhs of Eq. (3.2) are relatively more important for the 2^+, $T=1$ transition than for the 2^+, $T=0$ transition. Furthermore, the better agreement of the DREX calculations suggests that these current-current contributions are physically accurate.

Careful study of Fig. 3 reveals that a slight increase in the strength of the exchange contributions would result in

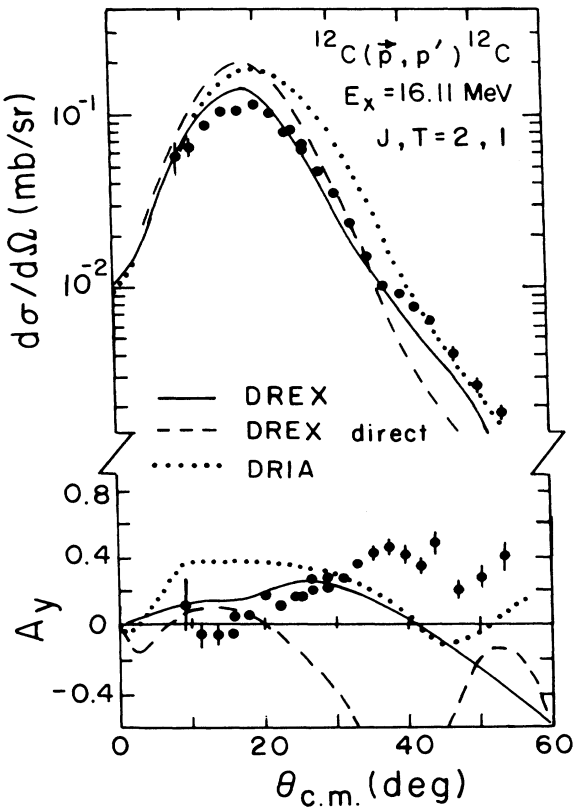

FIG. 3. Relativistic DREX calculations (solid line) are compared with the data from Ref. 14 for excitation of the 16.11 MeV 2^+, $T=1$ state in ^{12}C by 200 MeV protons. Also shown are DREX calculations with only a direct term (dashed line) and a nonexplicit exchange DRIA calculation (dotted line).

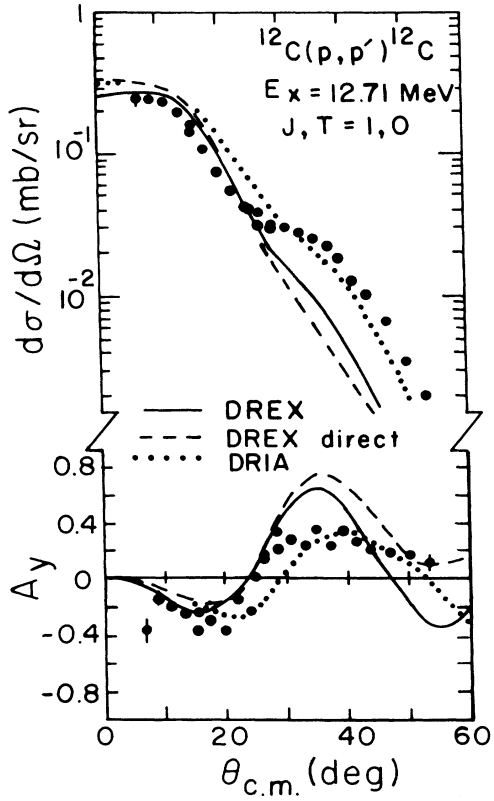

FIG. 4. Relativistic DREX calculations (solid line) are compared with the data from Ref. 14 for excitation of the 12.71 MeV 1^+, $T=0$ state in ^{12}C by 200 MeV protons. Also shown are DREX calculations with only a direct term (dashed line) and a nonexplicit exchange DRIA calculation (dotted line).

a global improvement in the agreement with data. For example, the maximum in the cross section at $\theta\simeq 20°$ is substantially reduced by the exchange contribution, but still further reduction is required for optimum agreement with experiment. Similarly, exchange increases the cross section at $\theta\simeq 40°$, but not enough. (Similar but smaller effects are also observed for the 2^+, $T=0$ cross section.) Also, at $\theta\simeq 40°$, exchange causes the analyzing power to become much more positive, but the data are more positive still.

In the remainder of this section, we will consider the unnatural parity 12.71 MeV 1^+, $T=0$ and 15.11 MeV 1^+, $T=1$ transitions. Figures 4 and 5 present 200 MeV cross section and analyzing power data compared with DREX and DRIA calculations. The large experimental differences between the $T=0$ and $T=1$ cases are again qualitatively reproduced in both sets of calculations. (In contrast, nonrelativistic calculations[14,21,22] typically fail to describe the 1^+, $T=0$ cross section data at $T_p \lesssim 200$ MeV.) We also observe that, for cross sections at $\theta < 22°$, theory and experiment are in quantitative agreement, DREX vs DRIA differences are small, and DREX exchange contributions are minor. However, for $\theta > 22°$, large DREX vs DRIA differences are found *even though* the DREX exchange contribution appears to be small. This suggests a cancellation between the exchange contributions corresponding to the lowest order term on the rhs of Eq. (3.2) which are present in both DREX and DRIA and the current-current contributions (plus higher order terms) absent in DRIA. The DREX vs DRIA differences are greatly magnified in the analyzing power results and again are larger than the size of the DREX exchange contributions would suggest. It is interesting that, for three of the four observables shown in Figs. 4 and 5—the exception being the $T=1$ cross section at large angles—the DRIA results are in *better* agreement with the data than the full DREX calculations. This is most dramatically illustrated by the 1^+, $T=1$ analyzing power (Fig. 5). Here the DRIA provides a good description of the data, especially for $\theta < 22°$, where the cross section is also well reproduced. The DREX direct-only result is almost exactly equal and *opposite* the data and the exchange contribution, though appreciable, moves the calculation only part way toward the DRIA calculation and the data. This again suggests cancellations between the terms in Eq. (3.1) which are implicitly present in the DREX exchange integrals. However, in contrast to the findings for the 2^+, $T=1$ transition discussed above, the disagreement between the DREX results

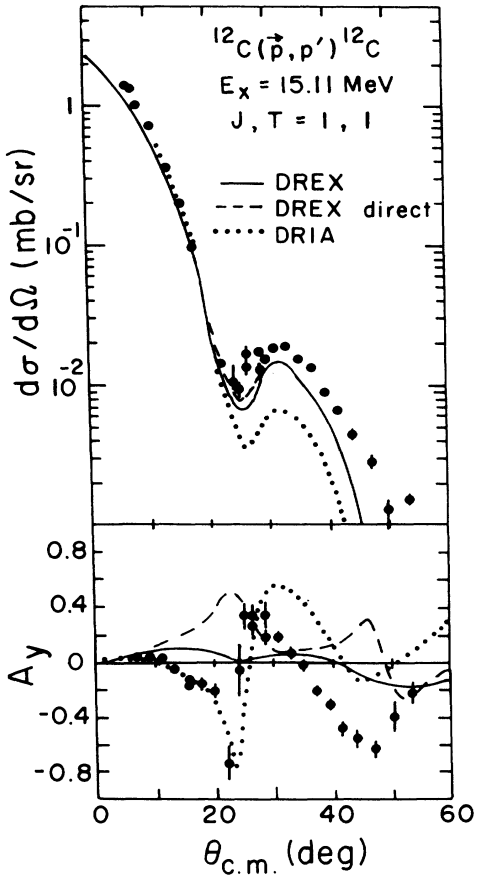

FIG. 5. Relativistic DREX calculations (solid line) are compared with the data from Ref. 14 for excitation of the 15.11 MeV 1^+, $T=1$ state in ^{12}C by 200 MeV protons. Also shown are DREX calculations with only a direct term (dashed line) and a nonexplicit exchange DRIA calculation (dotted line).

and the data taken together with the excellent agreement of the DRIA would seem to indicate that these cancellations are *unphysical.* This speculation is further supported by comparison of DREX and DRIA calculations with preliminary[23] $D_{ls}+D_{sl}$ data for the 1^+, $T=0$ transition at 200 MeV (we note that $D_{ls}+D_{sl}$ and $P-A_y$ are closely related).[8] Here the data are small and positive and very well described by the DRIA calculations while the DREX results, being large and negative, are in striking disagreement.

The main source of the disagreement with data can be traced to a single term in the (p,p′) amplitude. Using the language of Ref. 8, this term is labeled C_q and, in the direct-only picture of Ref. 8, it depends only on the time-like axial vector piece of the NN t matrix. In the Horowitz representation of the NN amplitude,[6] both the isoscalar and isovector axial-vector relativistic invariants are dominated by exchange contributions, as is documented in Table I where the exchange-to-direct ratio is displayed. Furthermore, these exchange contributions come predominantly from long-range pieces of the interaction as demonstrated in Table I. (We note that the "meson" contributing to the imaginary exchange amplitude is essentially the pion.) As discussed above, Eq. (3.3) suggests that, for a large "meson" mass, the current-current contribution will be small, the exchange t matrix can be factorized, and explicit treatment of exchange is unnecessary. Also, under these conditions, the ratio of the exchange to direct contributions should be the same in the (p,p′) amplitude as in the NN amplitude. Indeed this behavior is found for terms in the 2^+, $T=0$ amplitude where long-range "mesons" make negligible contributions to the relevant NN exchange amplitudes. Conversely, when long-range "mesons" play an important role, we anticipate large current-current contributions and the possibility of different exchange-to-direct ratios for NN compared to (p,p′). This anticipation is confirmed in Table I, where we observe that the exchange-to-direct ratio for C_q is uniformly *much* less than for the axial-vector invariant, $\hat{F}_A$. This effect is especially pronounced for the 1^+, $T=0$ transition where the imaginary part of the (p,p′) exchange amplitude is an order of magnitude *smaller* than the direct while for $\hat{F}_A$ it is about three times larger. This behavior largely explains the discrepancy with the $D_{ls}+D_{sl}$ data discussed above.

In studying a number of (p,p′) amplitudes for various transitions, we find that the exchange contribution is generally suppressed relative to the NN case by an amount which scales according to the proportion of the NN exchange contribution coming from long-range "mesons."

TABLE I. Direct and exchange contributions to the axial-vector invariant [in units of $(\mathrm{GeV}/c^2)^{-2}$] are presented at interesting kinematic values appropriate for the 200 MeV 1^+ excitations of Figs. 4 and 5 (viz., $\theta_{c.m.}=15°$ for the $T=0$ case and $\theta_{c.m.}=23°$ for the $T=1$ case). Since the full amplitude is $\hat{F}=\hat{F}^D-\hat{F}^X$, considerable cancellation is seen. The long-range exchange term is due to the $I=1$, pseudoscalar real and imaginary "mesons" of Ref. 6. The latter can be identified with one-pion exchange. The ratios of exchange to direct axial-vector amplitudes are compared with equivalent ratios in the (p,p′) amplitudes, C_q, as discussed in the text.

Level		$\hat{F}_A^D$	$\hat{F}_A^X$	$\hat{F}_A^X$ (long range)	$\hat{F}_A^X/\hat{F}_A^D$	C_q^X/C_q^D
$1^+, T=0$	real	−4.42	−1.47	−2.05	+0.74	−0.02
	imag	+1.94	+5.51	+4.48	−0.92	+0.09
$1^+, T=1$	real	+0.60	+1.31	+0.78	+1.42	+0.60
	imag	−1.17	−1.43	−1.92	+0.39	+0.06

It also seems that agreement with data is generally worsened by this suppression. This conclusion may have relevance beyond our RIA model of (p,p'). Such a speculation is suggested by the fact that, for the 1^+, $T=1$ analyzing power and 1^+, $T=0$ $D_{ls}+D_{sl}$ observable discussed above, standard nonrelativistic impulse approximation calculations[23]—where knockon exchange is in fact the dominant contribution—are nearly identical to the DREX results, indicating that both treatments may suffer from the same deficiencies.

At present, we cannot identify the source of the apparent problems with the current-current exchange contributions except that the difficulty probably lies in the NN interaction used. Remedies may involve lifting the requirement of a local representation for t_{NN}, using an extended form of t_{NN} which includes invariants which are zero on shell but contribute off shell,[24] or including medium effects. The possible relevance of medium effects is suggested by recent nonrelativistic g-matrix calculations for the 1^+, $T=1$ transition at 200 MeV (Ref. 25) which give an excellent description of A_y where the impulse approximation, as discussed above, fails badly. Investigation of these questions will be the subject of future work.

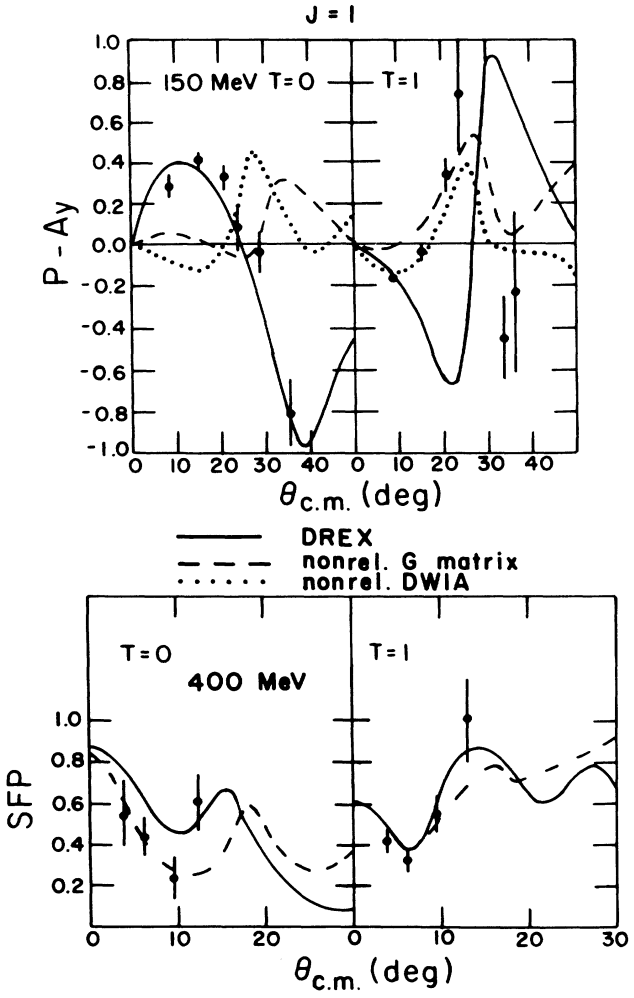

FIG. 6. Relativistic DREX calculations (solid line) and nonrelativistic reaction-matrix calculations (Ref. 21) are compared with data from Ref. 26 (150 MeV $P-A_y$) and Ref. 27 (400 MeV D_{nn}) for excitation of unnatural parity states in ^{12}C.

As a final comparison with data, we present in Fig. 6 some other spin-observable data for the 1^+ pair of excitations already discussed above. The $P-A_y$ observable has received considerable attention since it arises from "exotic" terms in the NN interaction. For example, in standard nonrelativistic treatments using local representations of the NN t matrix, knockon exchange contributions are required[19] to give nonzero $P-A_y$. In contrast, terms yielding nonzero $P-A_y$ arise quite naturally in a corresponding relativistic treatment[8,28] due essentially to the fact that the operator which gives the lower component of the four-component relativistic wave functions in terms of the upper is nonlocal. It is seen that the data[26] are well described by DREX for the $T=0$ transition at 150 MeV. The DRIA results are quite similar.[28] On the other hand, the $T=1$ case is poorly described, which reflects the same failure found in the A_y calculations of Fig. 5. Likewise, DRIA gives a *much* better description of the data, just as was the case for A_y at 200 MeV. (The apparent agreement of the DWIA nonrelativistic curve for the $T=1$ $P-A_y$ case is probably fortuitous since improved NN amplitudes give inferior fits.[29]) Other spin observables[29] (e.g., D_{nn}) are also poorly described by the DREX calculations for the $T=1$ transition at 150 MeV. However, it should be noted that nonrelativistic calculations also have difficulties at these energies (Fig. 6) and are very sensitive to the detailed form of the NN interaction[25,30] used.

At 400 MeV incident energy there is far better agreement with calculations and data,[27] as shown in the figure for a "typical" spin observable, namely the spin-flip probability, SFP$=\frac{1}{2}(1-D_{nn})$. Here, in keeping with the above discussion, the overall exchange contribution is relatively smaller in the DREX calculations and the differences between explicit (DREX) and nonexplicit (DRIA) treatments are smaller still.

IV. CONCLUSIONS

We have formulated a microscopic relativistic description of nucleon-nucleus inelastic scattering in which the knockon exchange contributions are treated explicitly. We have also constructed and tested a computer program to evaluate numerically the (p,p') amplitudes of our model. We use the antisymmetrized relativistic invariant amplitudes of Horowitz (Ref. 6) both for the NN interaction which drives the inelastic transition and to generate the nucleon-nucleus distorted waves. Both knockon exchange and Pauli-blocking effects are included in calculating the latter.

We have done an initial set of calculations for the lowest 2^+ $T=0$, 2^+ $T=1$, 1^+ $T=0$, and 1^+ $T=1$ transitions in ^{12}C at $T_p=200$ and 400 MeV. The 200 MeV calculations for the 2^+ $T=0$ transition are in excellent quantitative agreement with cross section and analyzing power data. For the other transitions, our results show reasonable agreement with experiment, comparable to or

better than standard nonrelativistic calculations.

Test calculations show that exchange contributions are generally small at a bombarding energy of 400 MeV. Differences between explicit (DREX) and implicit (DRIA) treatment of exchange are smaller still. At 200 MeV, knockon exchange contributions can be appreciable, and substantial differences between explicit and implicit treatments of exchange are found, especially for spin observables such as the analyzing power for the 15.11 MeV 1^+, $T=1$ transition in ^{12}C. Such differences can be attributed to so-called current-current terms implicitly included in the DREX calculations but absent in DRIA. There is some evidence, based on comparison with 200 MeV data for the 16.11 MeV 2^+, $T=1$ transition in ^{12}C, that these current-current contributions may be physically correct when they arise from relatively short-range pieces of the NN t matrix. However, comparison with data for the lowest 1^+, $T=0$ and $T=1$ transitions in ^{12}C suggests that such contributions coming from long-range pieces of t_{NN} substantially cancel the leading-order exchange amplitudes and that such cancellations are unphysical. The origin of this difficulty has not been identified and will be the subject of future investigations.

ACKNOWLEDGMENTS

We would like to thank W. G. Love for valuable discussions about the role of exchange contributions in (p,p'). We also gratefully acknowledge the support of the U.S. Department of Energy.

[1]J. A. McNeil, J. R. Shepard, and S. J. Wallace, Phys. Rev. Lett. **50**, 1439 (1983).
[2]J. R. Shepard, J. A. McNeil, and S. J. Wallace, Phys. Rev. Lett. **50**, 1443 (1983).
[3]E. Rost, J. R. Shepard, E. R. Siciliano, and J. A. McNeil, Phys. Rev. C **29**, 209 (1984).
[4]J. R. Shepard, E. Rost, and J. Piekarewicz, Phys. Rev. C **30**, 1604 (1984).
[5]L. G. Arnold, B. C. Clark, and R. L. Mercer, Phys. Rev. C **19**, 917 (1979); L. G. Arnold, B. C. Clark, R. L. Mercer, and P. Schwandt, *ibid.* **23**, 1949 (1981).
[6]C. J. Horowitz, Phys. Rev. C **31**, 1340 (1985).
[7]D. Murdock and C. J. Horowitz, in *Antinucleon- and Nucleon-Nucleus Interactions,* edited by G. D. Walker, C. D. Goodman, and C. Olmer (Plenum, New York, 1985), p. 135.
[8]J. R. Shepard, E. Rost, and J. A. McNeil, Phys. Rev. C **33**, 634 (1986).
[9]J. Raynal, Nucl. Phys. **A97**, 572 (1967).
[10]L. Wolfenstein, Annu. Rev. Nucl. Sci. **6**, 43 (1956).
[11]R. A. Arndt and D. Roper, Virgina Polytechnic Institute and State University Scattering Analysis Interactive Dialin program and data base.
[12]M. Abramowitz and I. A. Stegun, *Handbook of Mathematical Functions* (Dover, New York, 1970).
[13]J. D. Bjorken and S. D. Drell, *Relativistic Quantum Mechanics* (McGraw-Hill, New York, 1964).
[14]J. R. Comfort *et al.*, Phys. Rev. C **26**, 1800 (1982); **21**, 2147 (1980); **24**, 1834 (1981).
[15]C. J. Horowitz and B. D. Serot, Nucl. Phys. **A368**, 503 (1981).
[16]C. W. deJager, H. deVries, and C. deVries, At. Data Nucl. Data Tables **14**, 479 (1974).
[17]S. Cohen and D. Kurath, Nucl. Phys. **73**, 1 (1965); T. H. S. Lee and D. Kurath, Phys. Rev. C **21**, 293 (1980).
[18]The NN amplitudes are fit to a sum of five Yukawa forms with fixed masses as discussed in Ref. 4. It should be noted that this fit is constrained only for angles less than 60° in the NN system (or about 30° in the nucleon-nucleus system).
[19]W. G. Love and J. R. Comfort, Phys. Rev. C **27**, 2123 (1983).
[20]W. G. Love and A. Klein, in Proceedings of the LAMPF Workshop on Dirac Approaches to Nuclear Physics, edited by J. R. Shepard, C.-Y. Cheung, and R. L. Boudrie, Los Alamos National Laboratory Report LA-10438-C, 1985, p. 220.
[21]L. Rikus, K. Nakano, and H. V. vonGeramb, Nucl. Phys. **A414**, 413 (1984).
[22]W. Bauhoff *et al.*, Nucl. Phys. **A410**, 180 (1983).
[23]C. Olmer, in *Antinucleon- and Nucleon-Nucleus Interactions* edited by G. Walker, C. D. Goodman, and C. Olmer (Plenum, New York, 1985), p. 261; and private communication.
[24]J. A. Tjon and S. J. Wallace, Phys. Rev. C **32**, 267 (1985); **32**, 1667 (1985); University of Maryland Report 87-003, 1986.
[25]W. G. Love and A. Klein, in Proceedings of the Sixth International Symposium on Polarization Phenomena in Nuclear Physics, Osaka, 1985, p. 78.
[26]T. A. Carey *et al.*, Phys. Rev. Lett. **49**, 266 (1982).
[27]S. J. Seestrom-Morris *et al.*, Phys. Rev. C **26**, 2131 (1982).
[28]D. A. Sparrow *et al.*, Phys. Rev. Lett. **54**, 2207 (1985).
[29]M. Kovash (unpublished).
[30]W. G. Love and M. Franey, Phys. Rev. C **24**, 1073 (1981).